THE DEVELOPMENT OF A METHOD TO PREDICT THE CONTAMINANT CAPACITIES OF LOW MICRON, WOVEN STAINLESS STEEL FILTER ELEMENTS

By

ROGER HARRELL TUCKER

Bachelor of Science

Oklahoma State University

Stillwater, Oklahoma

1961

Submitted to the Faculty of the Graduate School
of the Oklahoma State University
in partial fulfillment of the requirements
for the degree of
MASTER OF SCIENCE
May, 1963

THE DEVELOPMENT OF A METHOD TO PREDICT THE CONTAMINANT CAPACITIES OF LOW MICRON, WOVEN STAINLESS STEEL FILTER ELEMENTS

Thesis Approved:

Thesis Adviser

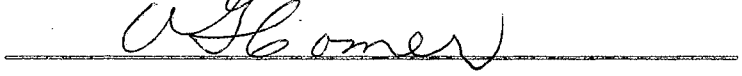

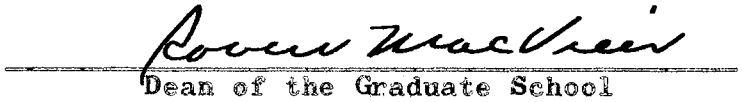

Dean of the Graduate School

ACKNOWLEDGMENTS

I would like to take this opportunity to express my sincere appreciation to the following individuals who aided my progress in this study:

To Dr. J. H. Boggs, Head of the School of Mechanical Engineering, for the research assistantship which I have held during the past year.

To Professor E. C. Fitch for his guidance and encouragement in the preparation of this thesis.

To my fellow research assistants, R. E. Reed, J. E. Bose, D. M. DeMoss, R. E. Bose, and C. R. Gerlach, for their willing cooperation and assistance in this study.

To the personnel of the Mechanical Engineering Laboratory for their technical advice.

To my parents for their encouragement in this endeavor.

To my wife, Patricia, for the understanding and help which she has provided throughout my graduate study.

TABLE OF CONTENTS

LIST OF TABLES

LIST OF FIGURES

CHAPTER I

INTRODUCTION

The development, in recent years, of complex and miniature hydraulic control systems has brought with it a number of problems which previously had not existed. One of the principle problems which has arisen is the necessity of obtaining a hydraulic fluid whose contamination concentration is compatable with the clearances of the control system components.

In order to obtain the quality of fluid required for satisfactory operation of such systems, better methods of filtration have been developed. The paper filter element, commonly used, has been discarded in many cases for more reliable elements constructed from a finely woven stainless steel wire. However, this improvement in quality brought with it a corresponding increase in the price of an element.

To justify the increased price required for stainless steel filter elements, methods have been and are being developed to clean them to a serviceable condition. However, the cost of such cleaning procedures is also a significant expense, often amounting to as much as one-fourth of the cost of a new element. Hence, for economy, it is desirable that the filter element be left in service until its contaminant holding capacity is virtually lost.

The procedure usually followed to determine the contaminant

holding capacity of an element has been to inject known weights of a standard artificial contaminant into the fluid, upstream of the filter element being tested. These injections are continued up to a point where the differential pressure across the element indicates that it is essentially "loaded". Obviously, this test is useless in determining whether or not an element may be continued in service since the remaining contaminant capacity of the filter has been usurped by the artificial contaminant.

Hence, it has been the attempt of the author to develop a test which will determine the available capacity of a filter element without destroying the usefulness of this capacity.

CHAPTER II

PREVIOUS INVESTIGATION

Although low micron, woven stainless steel filter elements are relatively new products, much of the theory and research which has been applied to other filter media is applicable in determining the properties of the wire cloth medium. In general, previous investigators have considered four properties which indicate the usefulness of a filter element. These properties include: the manner in which the filtration is carried out; the size of the largest particle which can pass through a given filter; the pore-size distribution for the element; and the filter area available for filtration which, in turn, governs the element's contaminant capacity.

It is generally agreed that woven stainless steel filters employ two methods of filtration. Hacker (1)[1] refers to these two methods of filtration as surface and depth filtration. In surface filtration the element acts as a sieve, retaining all particles larger than the pores in the filter. For this type of filter the number of pores available for clogging determines the contaminant capacity of the element. For this reason, elements of this type are usually formed by convoluting the surface of the

---

[1]Parentheses refer to Selected Bibliography.

filter to provide a large filtration area in a minimum volume. In depth filtration the element media is a labyrinth of flow passages, into which the particles of contamination pass and are trapped. Of these two types, surface filtration is the primary method active in wire cloth elements, since the element consists of only one layer of wire cloth. However, the weaving process does yield some of the characteristics of a depth filter because of the tortuosity of the fluid flow path. (2).

Another property by which the usefulness of a filter element is evaluated is the size of the maximum particle which will pass through the medium. Grace (3) outlines a test which has been widely used to determine the radius of the maximum round pore in a porous medium. The test consists of submerging the element in a liquid and increasing the air pressure inside of the filter until an air bubble appears. Using the pressure of the air inside of the element at this point and the characteristics of the liquid being used, the radius of the maximum pore size may be calculated from the following formula:

$$D_m = (0.0209) \frac{\sigma \cos \theta}{P_b} \quad . \qquad (2\text{-}1)$$

Pall (2) has applied a similar test to determine the size of the largest spherical particle which will pass through the wire cloth manufactured by Aircraft Porous Media. This cloth, which has been trademarked "Regimesh", is woven in a pattern which is referred to as Dutch twill. In this type of weave the pores are triangular in shape. Therefore, it was necessary to revise the "bubble test" outlined by Grace (3) in order to compensate for

the deviation from round pores. In order to determine the effect of a change in the shape of the pores, Pall first measured the "bubble point" pressure, P_b, for a number of elements having "Regimesh" as the filter media. Following this, he measured the size of the largest spherical particle which passed through the respective filters. On the basis of the experimental results, he proposed the following formula:

$$D_m = \frac{238}{P_b} \quad . \qquad (2\text{-}2)$$

His results showed that equation (2-2) is valid for pore diameters ranging from 8 to 40 microns, providing that ethyl alcohol is used as the test liquid.

While the size of the largest particle which will pass through a filter medium is important, the quantities and sizes of the smaller particles which pass through the element are equally important. One approach used in predicting such behavior is the determination of the pore-size distribution for a given filter medium. For surface filters the pore-size distribution is defined as the pore area per unit of total filter area for a given pore size range, while for depth filters the distribution is defined in terms of the capillary and total filter volumes.

One of the first methods used for obtaining the pore-size distribution of a porous material was introduced by Washburn (4). In this test the evacuated porous sample is submerged in a non-wetting liquid such as mercury. As the pressure on the fluid is increased, a unique curve of cumulative mercury volume in the test sample versus pressure is obtained. Since the volume of fluid

entering the sample is a function of the pore radius as the pressure is increased, it was possible for Drake and Ritter (5) to derive the following equation representing a distribution function of pore size:

$$D(r) = \frac{\bar{P}}{RV_0} \frac{d(\Delta V)}{d\bar{P}} \quad . \qquad (2\text{-}3)$$

The assumption of circular pores in the medium is the primary error limiting the application of the above equation to wire cloth filters.

The French engineer, Henri Darcy, was perhaps the first person to develop a theory concerning the flow of fluids through porous media. He found that the velocity of flow through any porous media was proportional to the pressure drop per unit length and inversely proportional to the viscosity of the flowing fluid. He expressed his findings in the following equation:

$$V = \frac{K}{\mu} \frac{dp}{dl} \quad . \qquad (2\text{-}4)$$

The proportionality constant K, in equation (2-4), is referred to as the permeability of the porous medium and is a measure of the resistance of the medium to fluid flow. Although Darcy worked with flow through sand filters used in city water systems, his conclusions have been applied equally well to flow through other porous media, especially to the flow of fluids in oil and natural gas reservoirs. In reference to modern filtration media, equation (2-4) may be more readily applied to describe flow through depth filtration media, rather than surface filtration media.

Rainard (6), on the basis of data which were obtained in

correlating air permeability in textiles, proposed the following empirical formula:

$$\Delta P = C_1 Q^2 + C_2 Q \quad . \tag{2-5}$$

Although the data were insufficient to determine the exact nature of the constants, C_1 and C_2, it was suggested on theoretical grounds that they be given the following values:

$$C_1 = \frac{a \rho}{g_c (\pi NAR^2)^2} \cdot 10^{16} \tag{2-6}$$

and

$$C_2 = \frac{8L \mu}{g_c \pi NAR^4} \cdot 10^{14} \quad . \tag{2-7}$$

Grace (3) in criticizing Rainard's work indicated that the empirically determined value of C_1 might also be a function of the distribution of flow between interfiber and interyarn pores. While Rainard's work may be valid, the lack of experimental verification in the work limits its research utility.

Cranston (7) also investigated the flow of fluids through porous materials. He applied Poiseuille's Law for flow through a single capillary to analyze the resistance of a filter to liquid flow. Poiseuille's Law for a cylindrical capillary is expressed in the following manner:

$$Q = (3.4 \times 10^7) \frac{D^4}{\mu L} \Delta P \quad . \tag{2-8}$$

In order to extend equation (2-8) to cover the number of capillaries which are found in filter media, it was necessary for Cranston to combine a number of variables into a constant

characteristic of a given filter. Having done this, he arrived at equation (2-9).

$$Q = \frac{K_1}{\mu} \Delta P \quad . \tag{2-9}$$

The constant K_1, which he called the flow constant, is a function not only of the pore-size distribution, but also of the depth of the filter medium. Cranston's study represents one of the few theoretical developments regarding the methods of filtration in modern filter media. His application of Poiseuille's Law to filter media is one of the most significant contributions to the field of fluid filtration.

Seed and Fowle (8) also applied Poiseuille's Law to a theoretical treatment of the methods of filtration. Unlike Cranston (7), who took into account the pore-size distribution of the filter media, they assumed a mean pore radius in arriving at the following equation:

$$V = (2.125 \times 10^6) \frac{NAR^4}{\mu L} \Delta P \, . \tag{2-10}$$

In their experimental investigation, using paper elements, it was verified that the velocity of the flowing fluid varied inversely with the fluid viscosity. Seed and Fowle (8) further verified that the velocity was proportional to the filter area as predicted by equation (2-10). However, in investigating the velocity-pressure relationship, they discovered that the velocity was not directly proportional to the pressure drop across the element. Instead, the velocity was found to be proportional to the pressure raised to a power which varied from 0.63 to 0.91 for different

elements.

Lovett (9), in investigating flow-pressure relationships through wire mesh with Dutch weave, found that the following general equation might be used:

$$R = C(\Delta P)^k \quad . \tag{2-11}$$

In his work, Lovett defined the constants C and k for a number of sizes of wire mesh. An order of magnitude for these constants may be found in the example of the flow equation for a 65-micron mesh.

$$R = 3.0(\Delta P)^{0.54} \quad . \tag{2-12}$$

Since the elements investigated in this study are also manufactured with a Dutch weave, a flow equation may be expected which is similar in form to equation (2-11).

Casaleggi, et al. (10), have also observed that the pressure differentials across wire elements are not directly proportional to the rate of fluid flow through them. From their test results on 400 mesh (40-micron) screens, Figure 1, it may be determined that the flow rate and therefore the velocity of the fluid passing through the screen was proportional to the pressure differential raised to the 0.42 power.

As a part of their study, Casaleggi, et al., obtained pressure drop versus flow rate data as a function of the filter area. This was accomplished by preparing a small cylindrical filter unit and incrementally decreasing the area open to flow. These results, shown also in Figure 1, indicate that while the slopes of the pressure drop versus flow rate lines remain essentially

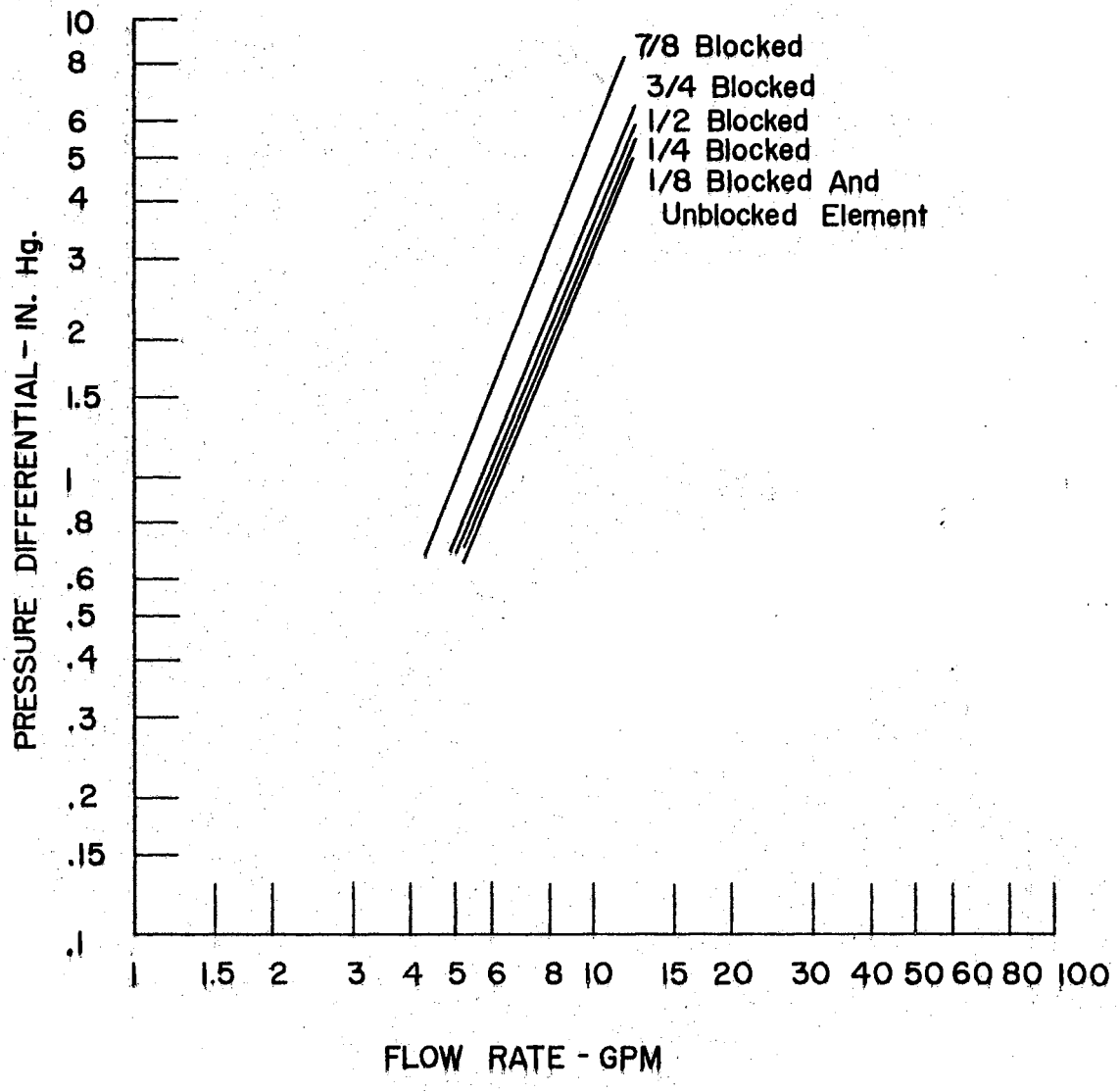

Figure 1. Pressure Drop Versus Flow Rate Data as a Function of Filter Area

constant, the lines are shifted in the direction of increasing pressure as the area decreases. In an attempt to compare these results with the actual contaminant capacity of the test element, the following assumptions were made regarding the filtration properties of the wire mesh.

1. Filtration takes place by sieving.
2. Particles of contaminant that are smaller than the pores of the screen pass through and the particles that are larger are trapped.
3. Each pore traps one particle.
4. When all the pores are clogged, the pressure drop will approach infinity.

Using these assumptions and knowing the number of pores per unit area and the number of particles above 40 microns per gram of an artificial contaminant (A.C. Coarse Dust), it was possible to calculate the number of grams of contaminant which would be necessary to close off a unit of filter area. Having theoretically determined the amount of contaminant necessary to produce the changes in flow area as shown in Figure 1, it was possible to prepare a theoretical contaminant capacity curve (Figure 2) for the test element. Figure 2 also contains the results of an actual contaminant capacity test conducted on an identical test element. A comparison of the actual and the theoretical curves indicates the validity of the assumptions which were made.

Personnel at General Dynamics (Convair) have conducted tests recently which are similar to those performed by Casaleggi, et al. (10). The contamination of a filter element was approximated by

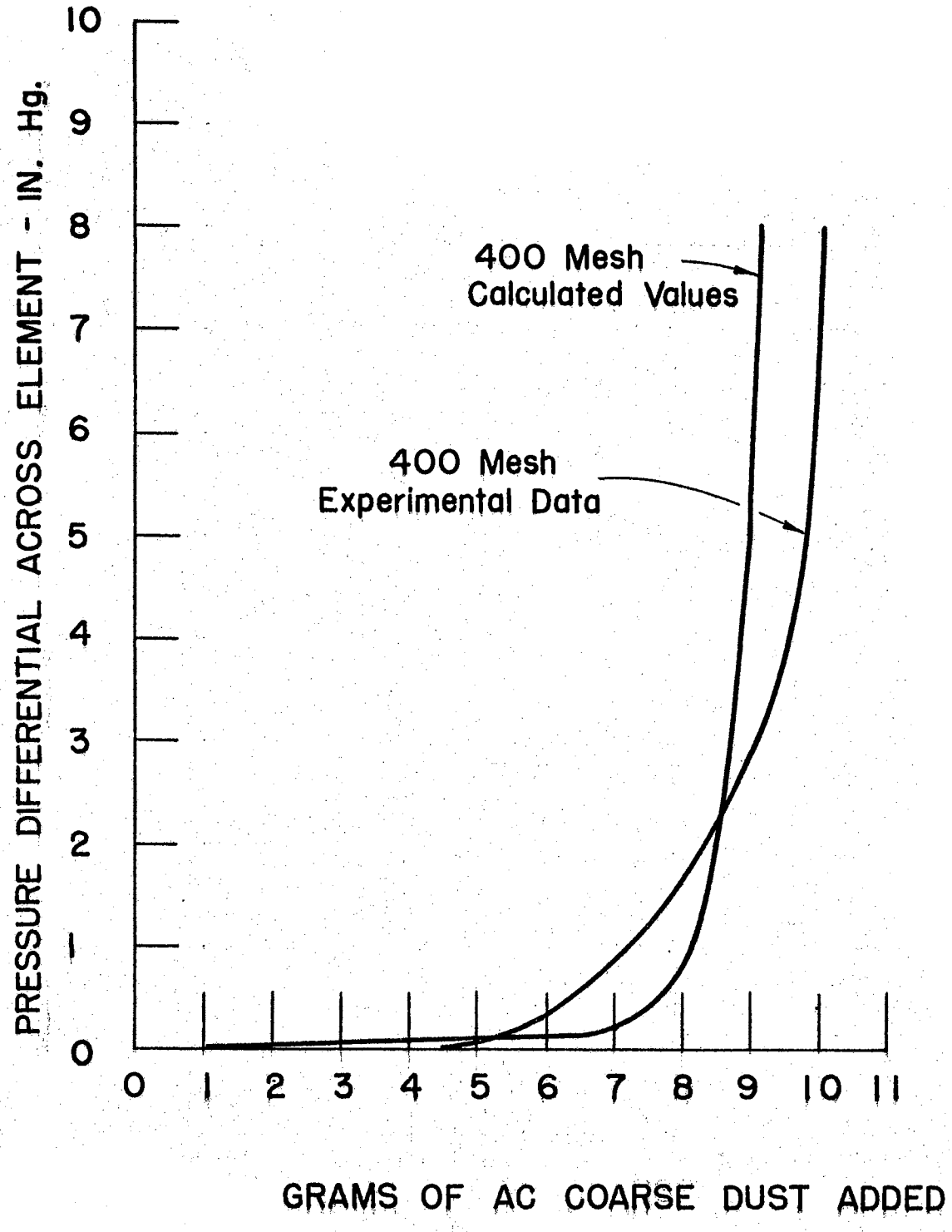

Figure 2. Comparison of Theoretical and Actual Contaminant Capacity Curves

incrementally closing the filter area with an epoxy resin. With each change in the area of the element a differential pressure was measured across the filter using both air and hydraulic oil as the test fluid. The test results (Figure 3) showed that a change in the relative filter area could be detected more readily by measuring the pressure when air was used as the test fluid than with the use of hydraulic oil.

Relying partially on these results, General Dynamics in 1956 initiated a program to check the effectiveness of the procedures being used to clean wire cloth filters on the B-58 aircraft. Following cleaning, each filter is placed on an adapter, and the pressure differential across it is measured at a given flow rate. On the basis of this pressure reading, the element is either judged clean and returned to service, or it is rejected, pending more extensive cleaning.

In 1961, personnel at the Filter Evaluation Laboratory at Oklahoma State University took part in a series of tests in conjunction with Tinker Air Force Base, Oklahoma, to determine the feasibility of using pressure drop versus flow rate tests to determine the relative contamination levels of a group of elements. (11). Identical tests were carried out at Tinker Air Force Base and at Oklahoma State University using the same test section and the same filters, in an attempt to standardize the procedures. After viewing the results (Figure 4) for an individual element, it was discovered that the viscosity of the fluid at Tinker Air Force Base (System 2) was 10 SSU lower than that of the fluid at Oklahoma State University (System 1). This indicated that strict

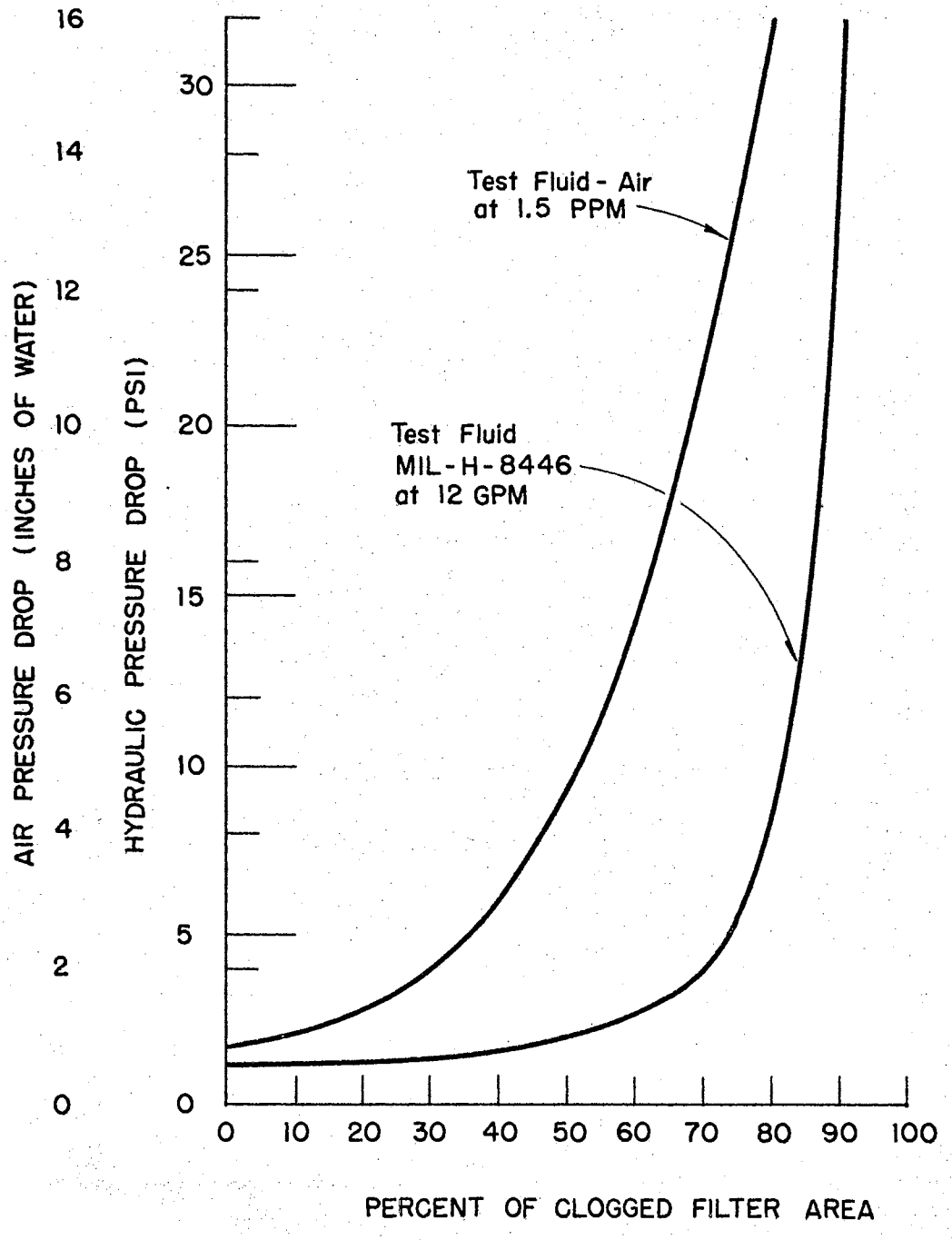

Figure 3. General Dynamic's Correlation Curve

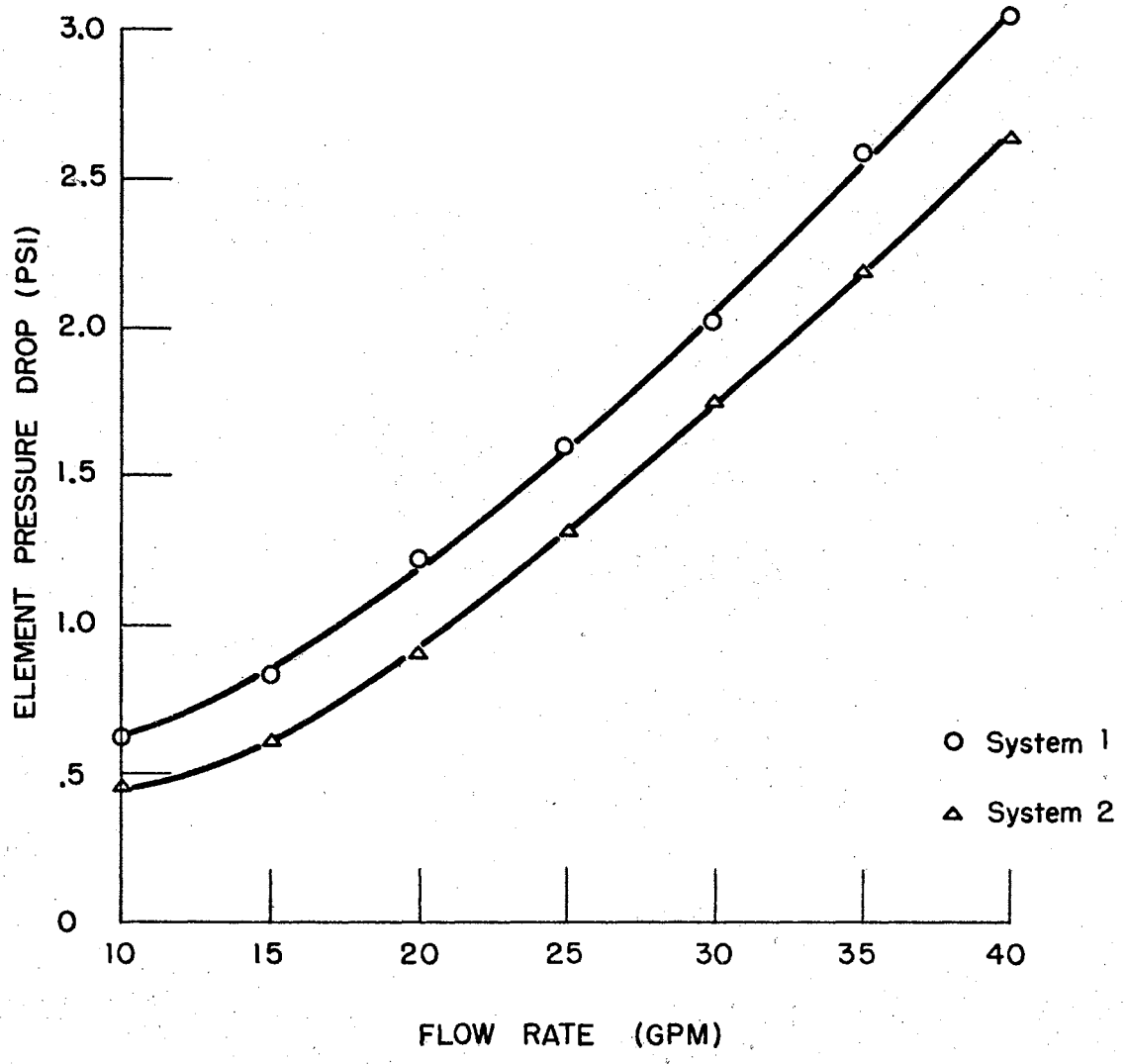

Figure 4. Pressure Drop Versus Flow Rate Data as a Function of Viscosity

viscosity control would be necessary in the standardization of pressure drop versus flow rate tests. The results also verified the pressure-viscosity relationships predicted by Darcy's equation (2-4) and Poiseuille's Law (2-8).

Based on the indicated success of General Dynamic's filter evaluation program, and because hydraulic pressure drop is sensitive to viscosity changes, air was selected as the test fluid to be used in future filter evaluation studies.

CHAPTER III

STATEMENT OF PROBLEM

The objective of this study was to develop a method to predict the contaminant capacities of low micron, woven stainless steel filter elements. In meeting this objective, an equation was derived containing a constant which is proportional to a filter's contaminant capacity. This constant was experimentally determined and compared with the actual capacity of a number of filters in order to determine a correlation.

CHAPTER IV

THE DEVELOPMENT OF AN EQUATION DESCRIBING THE CONTAMINANT CAPACITY OF A FILTER ELEMENT

In comparing the works of those cited in Chapter II, several factors become apparent regarding the relationships between the properties of porous media and of the fluids passing through such media. The effects, which variations in the filter media and fluid properties have on the pressure differential across a filter element, may be outlined in the following statements:

1. As the rate of fluid flow through an element is increased, the velocity of the fluid is increased, thereby increasing frictional loss or pressure drop through the filter.
2. The pressure differential across an element is proportional to the number of pores in the medium. Therefore, a decrease in the number of pores subjected to a constant flow rate results in a greater fluid velocity through the individual pores and a greater pressure drop.
3. A decrease in the sizes of a given number of pores, subjected to a constant flow rate, also causes an increase in the pressure differential across an element.

4. As the viscosity of the fluid passing through the filter is decreased, the frictional losses in the porous medium are decreased. This is observed as a decrease in the pressure loss across the element.
5. The differential pressure across a filter is a function of the depth of the element pore spaces, increasing as the length of the pore capillary is increased.

These relationships may be stated mathematically in the following expression:

$$P_f = K_2 \mu Q_f^s \sum_{i=1}^{n} \frac{L_i}{A_{pi}^2} \quad . \tag{4-1}$$

With one exception, equation (4-1) may be considered to be an extension of Poiseuille's Law (2-8) to cover n capillaries with varying depths and areas. This exception is in the flow rate term, Q_f, which has been raised to the s power as suggested by Seed (8), Casaleggi, et al. (10), and Lovett (9).

Assuming that the viscosity of the test fluid can be maintained at a constant value, equation (4-1) may be reduced to a new form.

$$P_f = K_3 Q_f^s \sum_{i=1}^{n} \frac{L_i}{A_{pi}^2} \quad . \tag{4-2}$$

The expression in this form still contains three variables which describe the filter media. These variables include: the number of pores available for filtration; the individual areas of each of these pores; and the depth or length of the pores.

Since each of these variables has an effect on the filtration method of a given filter media, the term containing them will be combined into a constant, characteristic of an individual element's filtration capacity. In doing this a new quantity, C_f, the filter capacity constant, will be defined. Equation (4-2) may then be written in the following manner:

$$P_f = \frac{Q_f^s}{C_f} \quad . \tag{4-3}$$

Comparing equations (4-3) and (4-2), the filter capacity constant can be found by the expression,

$$C_f = \frac{1}{K_3} \sum_{i=1}^{n} \frac{A_{pi}^2}{L_i} \quad . \tag{4-4}$$

In considering the effects of the properties of the filter medium upon the capacity constant, C_f, it should be noted that the capacity increases as the number of pores increase. Further, as the areas of the pores increase, the filter capacity increases. This statement appears, at first, to be a contradiction, since more particles pass through a filter as its pores are enlarged. However, a filter's capacity is defined as the weight of a graded contaminant which must be added to the filter to increase the pressure differential across it to a predetermined value. On the basis of this definition, the filter capacity increases with an increase in pore area. The third filter property involved in expressing the filter capacity constant is the length of the individual pores. As these lengths increase, the tortuosity of the

flow paths increase, and smaller particles are trapped in the filter. While the filtration efficiency of the filter increases with an increase in the pore lengths, its defined capacity decreases since it is removing smaller particles.

The evaluation of the filter capacity constant, C_f, requires a test facility on which pressure drop versus flow rate tests may be carried out for individual elements. Recalling the assumptions made in deriving equation (4-3), the viscosity of the fluid used in such a test facility must be maintained at a constant value. This is of primary importance in all tests to permit a comparison of the data.

The pressure drop and flow rate data obtained from a test on a given filter may be expressed as a straight line relating $Ln(P_f)$ versus $Ln(Q_f)$. The equation expressing this relationship is

$$Ln(P_f) = m\ Ln(Q_f) + b \quad . \tag{4-5}$$

By rearranging equation (4-5) and taking antilogarithms the expression becomes

$$P_f = Ln^{-1}(b)\ Q_f^{\,m} \quad . \tag{4-6}$$

Comparing equations (4-6) and (4-3), it may be seen that the exponent, s, is equal to the slope, m, of the $Ln(P_f)$ versus $Ln(Q_f)$ curve. The comparison also shows that,

$$C_f = \frac{1}{Ln^{-1}(b)} \quad . \tag{4-7}$$

In order to determine the effectiveness of using the filter capacity constant to indicate an element's capacity, it is

necessary to conduct contaminant capacity tests on a group of elements. As stated previously, contaminant capacities of filters are obtained by adding accurately weighed samples of a standard contaminant to the fluid upstream of the filter being tested. The element's capacity is then defined as the weight of contaminant which was added before the pressure differential across the element reached a predetermined reference value. The contaminant capacities of a group of elements may then be compared with their individual capacity constants, to determine the validity of equation (4-3).

CHAPTER V

THE DESIGN AND OPERATION OF THE AIR PERMEAMETER

In order to experimentally determine the value of the filter capacity constant (equation 4-4), it was necessary to meet the requirements outlined in Chapter IV. In meeting these requirements it was first necessary to select a test fluid, whose viscosity could be maintained at a constant value throughout the test program. Hydraulic oil was eliminated from consideration because of the strict temperature control which is required to maintain the viscosity of the oil at a set value. Another disadvantage which limits the use of hydraulic oil for such tests is the fact that its viscosity gradually decreases as the oil becomes worn. To obtain the viscosity control required, air was selected as the test fluid, since its viscosity is virtually independent of temperature.

After selecting the test fluid, a device was constructed to satisfy the requirements for a test facility. This device, called the Air Permeameter (Figures 5 and 6), is an apparatus designed to measure the differential pressure across a filter element concurrently with a measurement of the volume of air flowing through the element. To perform this test the filter is placed on an adapter in the bottom of an aluminum canister. Filtered air is then admitted through a port in the bottom of the canister and directed

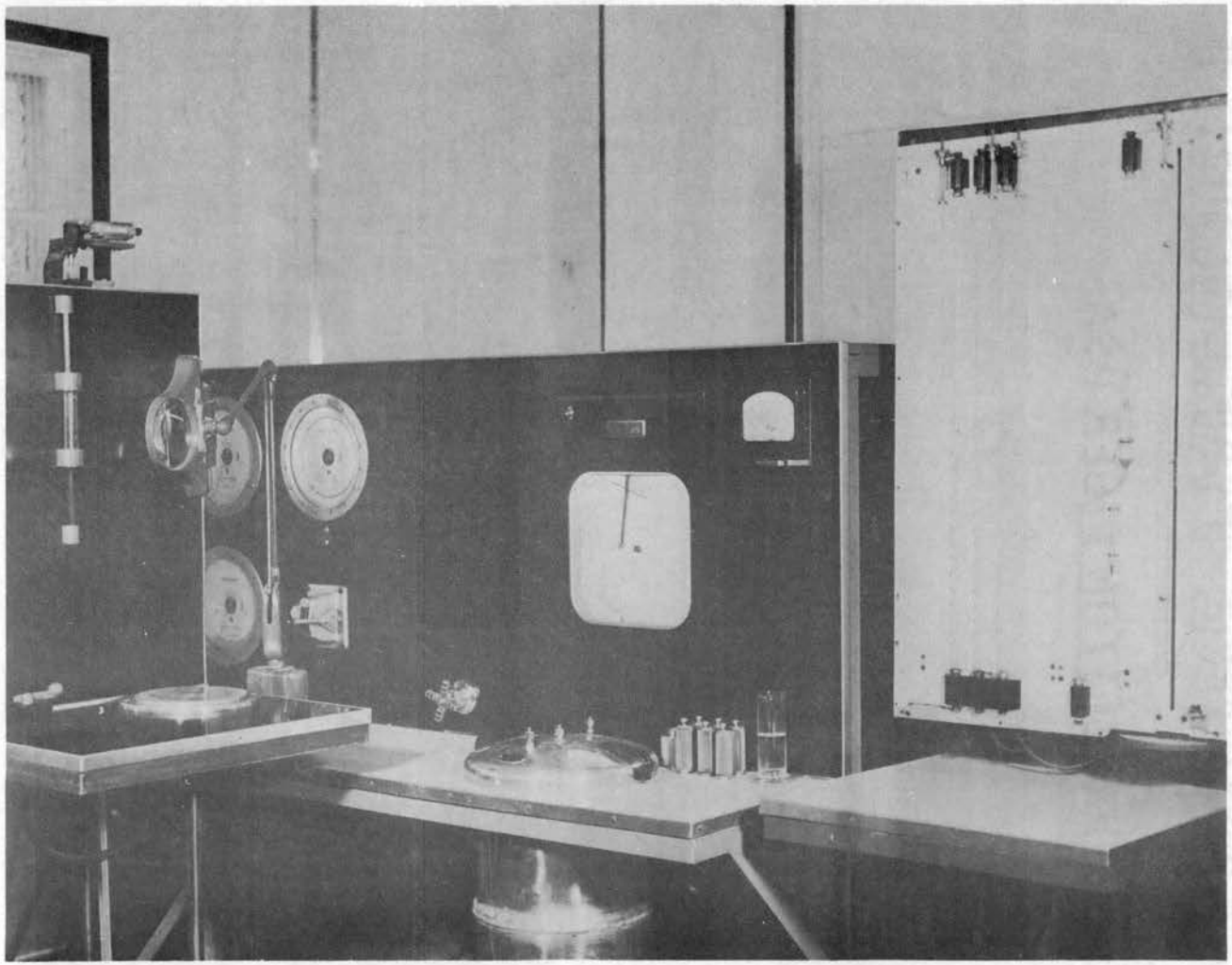

Figure 5. Air Permeameter.

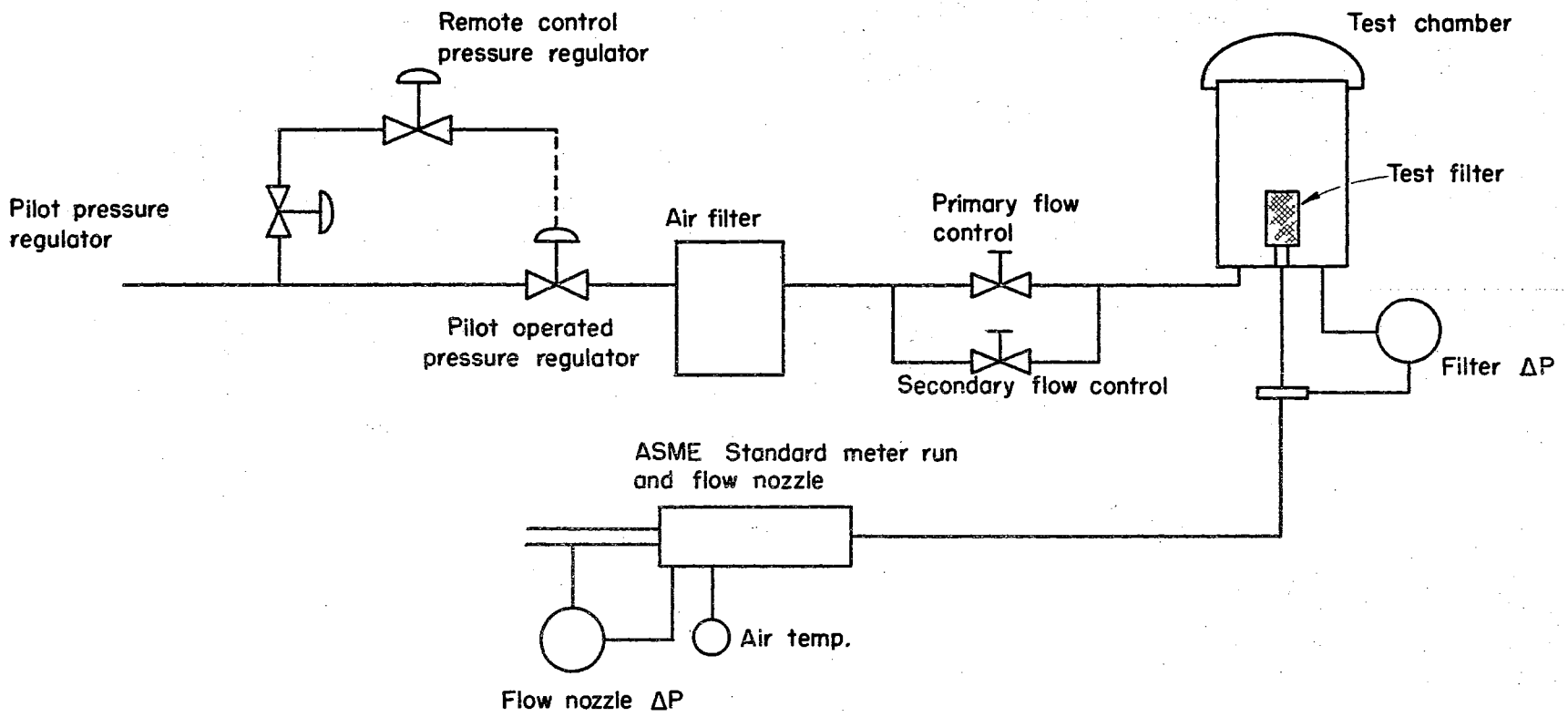

Figure 6. Schematic Diagram of Air Permeameter

toward the top of the container, where it is diffused before passing through the test element.

The differential pressure across the element is obtained by taking the high pressure reading from the inside of the tank, and by taking the low pressure reading through a piezometric ring downstream from the filter. To avoid dynamic effects on the low pressure reading, caused by changes in the flow patterns through various elements, it was necessary to construct and install a flow straightener in the pipe immediately downstream from the filter element. Hence, what is referred to as the pressure drop across the element is actually a combination of the losses across the element, the adapter associated with a given type of filter, and the flow straightener section. These additional losses, although significant, do not negate the pressure drop contribution of the filter.

In order to reach the accuracy required for the pressure drop measurement across the test filter, a micromanometer was selected which had a differential pressure range of from 0 to 15 inches of water, and a readability of one-hundredth of an inch of water. Using this instrument, it was possible to repeat pressure readings for a given filter to within one-hundredth of an inch of water.

The second major instrumentation system in the Air Permeameter is involved in measuring the volume of air passing through the filter element. After consideration of both a rotameter and a Venturi meter, A.S.M.E. flow nozzles were selected because of their accuracy, availability, and flexibility of range. In order

to measure the flow rate, the nozzle is attached to the downstream end of a standard metering run containing straightening vanes, a temperature well, and an upstream pressure probe. The low pressure reading is taken from the throat of the nozzle.

The weight rate of flow through the element and ultimately through the flow nozzle can be calculated from the following formula:

$$w = 6.870\ C_n D_n^2 (P_a P_w / T_a)^{\frac{1}{2}} \quad . \qquad (5\text{-}1)$$

Since the operating range for each A.S.M.E. nozzle requires that pressure differentials across the nozzle vary from 10 to 40 inches of water, it was necessary to obtain an instrument which would give accuracy in this range comparable to the accuracy available in measuring the pressure losses across the test element. A survey yielded no commercial unit with the accuracy and range required. Therefore, a micromanometer, similar to the model already available, was constructed to meet these requirements. (Appendix A).

Using the test equipment outlined above, it was possible to obtain accurate and repeatable results in the measurement of pressure differentials across the test element and housing at a number of flow rates.

CHAPTER VI

RESULTS OF TESTS

To determine the relationship between the filter capacity constant of an element and the element's actual capacity, experimental tests were carried out on two groups of filters. The first of these groups was comprised of 16 elements, each having a 5-micron nominal rating and a rated flow of 8 gpm. The second group consisted of 10 elements each with a 10-micron nominal rating and a rated flow of 12 gpm. Both groups were manufactured by Aircraft Porous Media, and were constructed from "Regimesh".

In order to meet the test objectives outlined in Chapter IV, each element was tested on the Air Permeameter (Chapter V) to obtain pressure drop versus flow rate data. This data was then analyzed, with the aid of the digital computer (Appendix B), to determine the value of the filter capacity constant for each element. The results of these tests are shown in Table I.

Also shown in Table I are the results of the contaminant capacity tests for each element (Appendix C). These tests were conducted to provide a means to determine the effectiveness of using the filter capacity constant to predict an element's actual capacity.

Figure 7 shows a comparison between the filter capacity constants and the actual contaminant capacities for each element in

TABLE I

COMPARISON OF FILTER CAPACITY CONSTANTS
WITH ACTUAL CONTAMINANT CAPACITIES
(5 micron elements)

Serial Number	Filter Capacity Constant	Actual Contaminant Capacity (gms)
155	.672	1.41
256	.660	1.39
1132	.625	1.29
2354	.595	1.20
2811	.601	1.37
2987	.637	1.61
3023	.628	1.30
4752	.604	1.20
5303	.617	1.46
5491	.684	1.70
5508	.667	1.62
5586	.622	1.54
5711	.671	1.51
5955	.606	1.44
10329	.687	1.72
10972	.654	1.54

TABLE I (Continued)

(10 micron elements)

Serial Number	Filter Capacity Constant	Actual Contaminant Capacity (gms)
2	.668	1.17
7	.712	1.56
55	.763	2.06
1358	.744	1.81
1505	.735	1.80
1527	.766	1.99
1540	.727	1.76
1834	.760	1.83
2508	.742	1.80
3088	.751	1.77

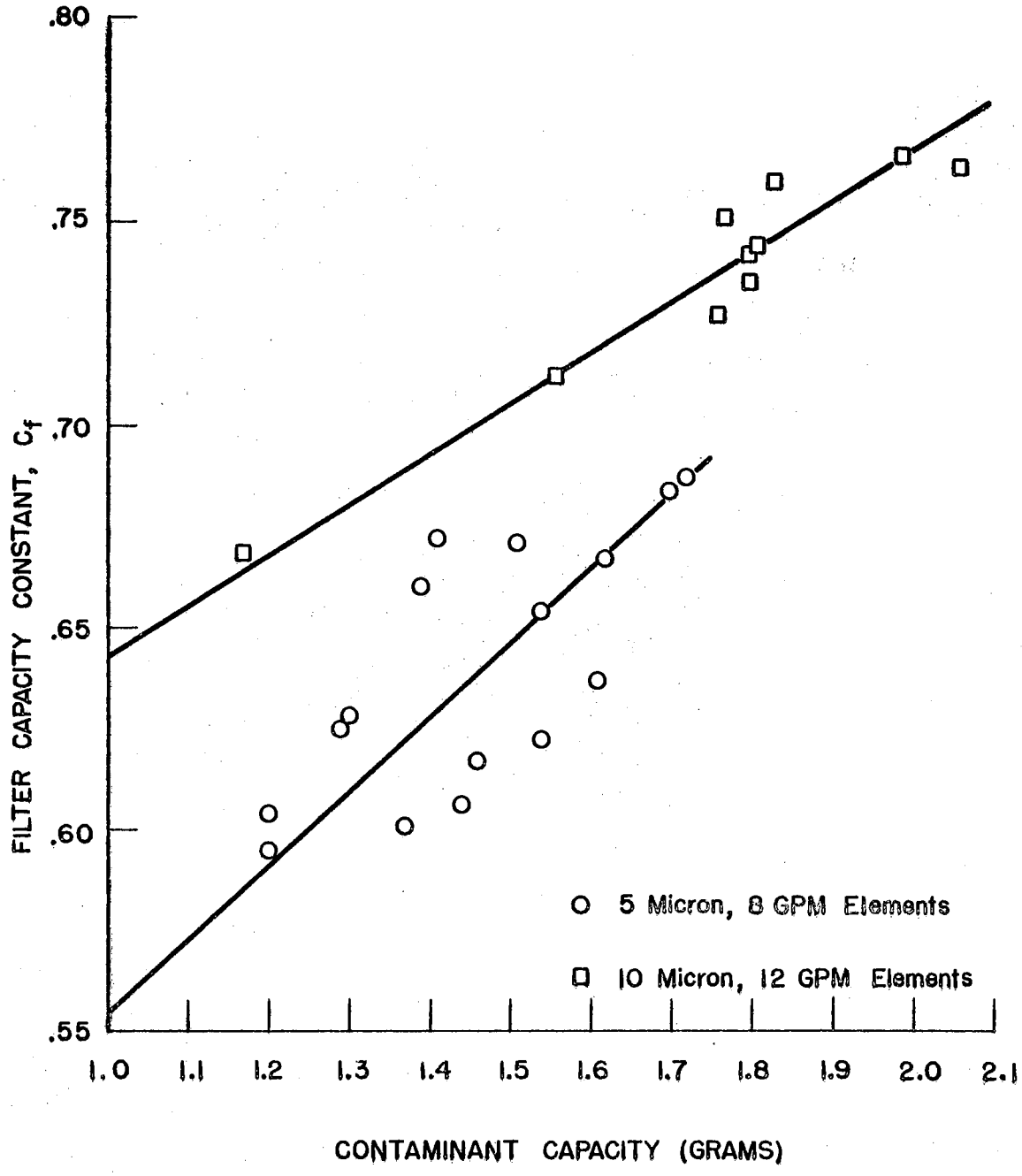

Figure 7. Correlation Between Filter Capacity Constant and Actual Contaminant Capacity

the two test groups. It may be seen from the two curves that the correlation was considerably better among the 10-micron elements than among the 5-micron elements. This was due, in part, to variations in the manufacturing procedures used to construct the 5-micron elements. The first elements of this type were made from a 10-micron wire cloth which had been rolled to obtain a 5-micron cloth. As the manufacturing process was improved, however, it became possible to weave a 5-micron mesh. These variations tended to make the results slightly erratic.

In Table II a comparison is made of the actual contaminant capacities with the values obtained from using the capacity constant and the correlation curves (Figure 7). These results show that the capacity constant was accurate to within 6 percent of predicting the actual contaminant capacity of each element tested in the 10-micron group. It may further be seen that the average deviation from the predicted value was only 2.3 percent. For the 5-micron elements, the maximum error was less than 11 percent, while the average error was 5.3 percent.

Errors may appear in these experimental results in several places. The first source of error exists in measuring the pressure drop across the filter element using the Air Permeameter. The pressure drop across the flow straightener in the Air Permeameter is a major contribution to the overall filter pressure drop. This factor possibly prevented the discovery of small differences between filters which appeared to be almost identical.

Another source of error existing in the Air Permeameter test is the condition of the element at the time of testing. Prior to

TABLE II

COMPARISON OF ACTUAL CONTAMINANT CAPACITIES WITH PREDICTED VALUES
(5 micron elements)

Serial Number	Actual Capacity (gms)	Predicted Capacity (gms)	Percent Error*
155	1.41	1.64	7.6
256	1.39	1.57	10.5
1132	1.29	1.39	5.8
2354	1.20	1.22	1.2
2811	1.37	1.25	7.0
2987	1.61	1.45	9.3
3023	1.30	1.40	5.8
4752	1.20	1.27	4.1
5303	1.46	1.34	7.0
5491	1.70	1.70	0.0
5508	1.62	1.61	0.6
5586	1.54	1.37	9.9
5711	1.51	1.63	7.0
5955	1.44	1.28	9.3
10329	1.72	1.72	0.0
10972	1.54	1.54	0.0
			5.3 Avg.

* Based on 1.72 gms total

TABLE II (Continued)

(10 micron elements)

Serial Number	Actual Capacity (gms)	Predicted Capacity (gms)	Percent Error*
2	1.17	1.20	1.5
7	1.56	1.55	0.5
55	2.06	1.97	4.4
1358	1.81	1.81	0.0
1505	1.80	1.74	2.9
1527	1.99	1.99	0.0
1540	1.76	1.68	3.9
1834	1.83	1.94	5.3
2508	1.80	1.80	0.0
3088	1.77	1.86	4.4
			2.3 Avg.

* Based on 2.06 gms total

each test, the element to be tested was soaked in petroleum ether to remove residual oil from the filter cloth. If the element were not allowed to dry adequately, after this soaking, any liquid which remained in the pores would have had the same effect as contaminant in the test results.

The contaminant capacity test is also subject to errors in several places. One of these is in the extrapolation of the contaminant capacity curves to the reference pressure (Appendix C). In some cases, the contaminant capacities obtained in this manner may be in error by as much as 0.5 grams. Another source for error in the contaminant capacity tests is in the control of the rate of injection of the contaminant. Test results indicate that as the rate of injection increases, the contaminant capacities appear to increase. This is due to the fact that the contaminated fluid is not thoroughly mixed before passing through the filter. Therefore, the contaminant is deposited unevenly on the filter. This leads to the buildup of a "filter cake" on certain regions of the filter and to an erroneous contaminant capacity.

A phenomenon, which has been noted in performing contaminant capacity tests, but not completely proven, is the variation of a filter's efficiency in removing particles as it becomes contaminated. It has been commonly believed that as an element becomes contaminated its efficiency in removing particles is increased. This idea results from the theory that as a filter becomes contaminated, the larger pores fill up first and the filtration is then carried out by the smaller pores. It was discovered, by counting the number of particles passing through the filter, that

this theory is adequate up to the point at which the pressure begins to rise rapidly with increased filter contamination (Figure 12). At this point, the efficiency begins to decrease, indicating that some of the particles, which are not securely trapped, are being forced through by the increased differential pressure.

CHAPTER VII

CONCLUSIONS

The results from the Air Permeameter and contaminant capacity tests show that the filter capacity constant, C_f, in equation (4-3), may be used to predict the actual contaminant capacity of a filter. A comparison of the results of these two tests for two groups of filter elements showed that the average deviation of the actual contaminant capacity from the predicted value was 5.3 percent for the 5 micron elements. For the 10 micron elements the average error was decreased to only 2.3 percent. The accuracy of these tests may be improved even further by a more rigid control of the test procedures as indicated in Chapter VI.

As a result of this study, certain conclusions can be reached regarding the use of this method to predict the contaminant capacities of low micron, woven stainless steel filter elements. These conclusions are as follows:

1. The Air Permeameter provides an accurate means of predicting the contaminant capacity of a filter element.
2. Since the Air Permeameter provides a direct appraisal of an element's contaminant capacity, it may be readily applied to quantitatively determine the effect of various filter cleaning techniques.

3. Using the Air Permeameter, various evaluation programs can be conducted on hydraulic systems, where a knowledge of the contamination levels of the filters in the system is required.

Based on these conclusions the following advantages may be indicated for selecting the Air Permeameter test over conventional contamination detecting tests. These advantages are as follows:

1. The Air Permeameter test is a quick, clean method as opposed to the inherent problems associated with hydraulic test methods.
2. The instrumentation required for an Air Permeameter facility is considerably less expensive than the cost of a comparable hydraulic facility.
3. The use of available shop-air systems makes an installation of the Air Permeameter a minor consideration.
4. The Air Permeameter test leaves the element in a serviceable condition, since it does not destroy the available contaminant capacity of the filter.

With improvements and a more rigid evaluation, the use of the Air Permeameter may assume a position, in evaluating filter elements, equal to that of the bubble test and the contaminant capacity test.

CHAPTER VIII

RECOMMENDATIONS FOR FUTURE STUDY

One of the principle causes for inaccuracies in the test results appears to be in the number of particles which are passed by the test filter during the contaminant capacity tests. In future experiments it is recommended that a pore-size distribution be obtained for each element in order to permit a more accurate prediction of the actual contaminant capacity of a given element. As is shown in Figure 11, a small variation in the size range of the particles which are passed by the filter has a significant effect in terms of the weight of test dust required to reach the contaminant capacity of a filter.

Another factor which should be considered in future experiments is the contribution of the flow straightener and element adaptor to the differential pressure obtained using the Air Permeameter. Every attempt should be made to reduce this added pressure loss so that the differential pressure across the element can be the primary factor. A possible solution is the extention of the low pressure probe into the element, providing that the dynamic pressure effects can be eliminated.

Before any test of this type can be initiated on a production basis, it should be realized that standardized facilities must be constructed to permit a comparison of the results among various

test units. To improve the reliability of the test results, it will also be necessary to perform contaminant capacity tests on a much larger group of elements than were considered in this study.

A SELECTED BIBLIOGRAPHY

1. Hacker, C. H., "Evaluating Fluid-Filtering Media", Product Engineering, XXXI (November 28, 1960), pp. 29-40.

2. Pall, D. B., "Development of Filters for 400°F and 600°F Aircraft Hydraulic Systems", Wright Air Development Center Technical Report No. 56-249, (May, 1956).

3. Grace, H. P., "Structure and Performance of Filter Media", American Institute of Chemical Engineering Journal, II (September, 1956), pp. 307-336.

4. Washburn, E. W., "Note On a Method of Determining the Distribution of Pore Sizes in a Porous Material", Proceedings of the National Academy of Sciences, VII (April 15, 1921), pp. 115-116.

5. Drake, L. C., and H. L. Ritter, "Macropore-Size Distribution in Some Typical Porous Substances", Industrial and Engineering Chemistry, XVII (December, 1945), pp. 787-791.

6. Rainard, L. W., "Air Permeability of Fabrics", Textile Research Journal, XVI (October, 1946), pp. 167-170.

7. Cranston, R. W., "Filtration of Fine Particles", Aircraft Engineering, XXIV (June, 1952), pp. 154-159.

8. Seed, R. G., and A. A. Fowle, "A General Study of Diverse Filtration Phenomena With Possible Applications to Aircraft Fuel Filtration", Wright Air Development Center Report No. 54-181, (November, 1952).

9. Lovett, R. E., "How to Design Parts from Wire Mesh", Product Engineering, XXXIII (July 9, 1962), pp. 67-73.

10. Casaleggi, C., E. Ludwig, and H. L. Forman, "Evaluation of Low Pressure Aircraft Fuel Filters", Wright Air Development Center Technical Report No. 55-317, (September, 1953).

11. Fitch, E. C., et al., "Study in the Field of Fluid Contamination and the Methods Required to Restore and Evaluate the Contaminant Capacity of Used Filter Elements", Oklahoma State University Engineering Research, Fluid Contamination Project, Report No. 5, (August, 1962).

12. "Test Code for Displacement Compressors, Vacuum Pumps, and

Blowers", American Society of Mechanical Engineers Power Test Codes, (May, 1939).

13. Amyx, J. W., D. M. Bass, Jr., and R. L. Whiting, Petroleum Reservoir Engineering, New York: McGraw-Hill Book Co., 1960, pp. 338-339.

14. Fitch, E. C., et al., "Study in the Field of Fluid Contamination and the Methods Required to Restore and Evaluate the Contaminant Capacities of Used Filter Elements", Oklahoma State University Engineering Research, Fluid Contamination Project, Report No. 4, (September, 1961).

APPENDIX A

DESIGN OF THE OKLAHOMA STATE UNIVERSITY MICROMANOMETER MODEL 2

The Oklahoma State University Micromanometer, Model 2 (Figure 8), was patterned after a previous model constructed by the late Professor Bert S. Davenport. This manometer has a range of zero to forty-five inches of water and a readability of one-hundredth of an inch of water. The manometer is operated by lowering the manometer reservoir until the unknown pressure is balanced by the height of water in the pressure leveling chamber.

This is accomplished by first raising the reservoir, with no applied pressure acting upon it, until the meniscus of the water in the leveling chamber is just touching the point of a needle inside the chamber. This is the "zero point" or the point at which the fluid in the reservoir and the leveling chamber are at equal heights. The manometer scale, a Veeder-Root counter, is then set at zero.

As pressure is applied to the system, the reservoir is lowered on a threaded shaft which is driven by an electric motor. The shaft has ten threads per inch so that each revolution indicates one-tenth of an inch of travel of the reservoir. These revolutions are measured by the counter which has a 1:10 ratio built into it. Therefore, the counter serves directly as the

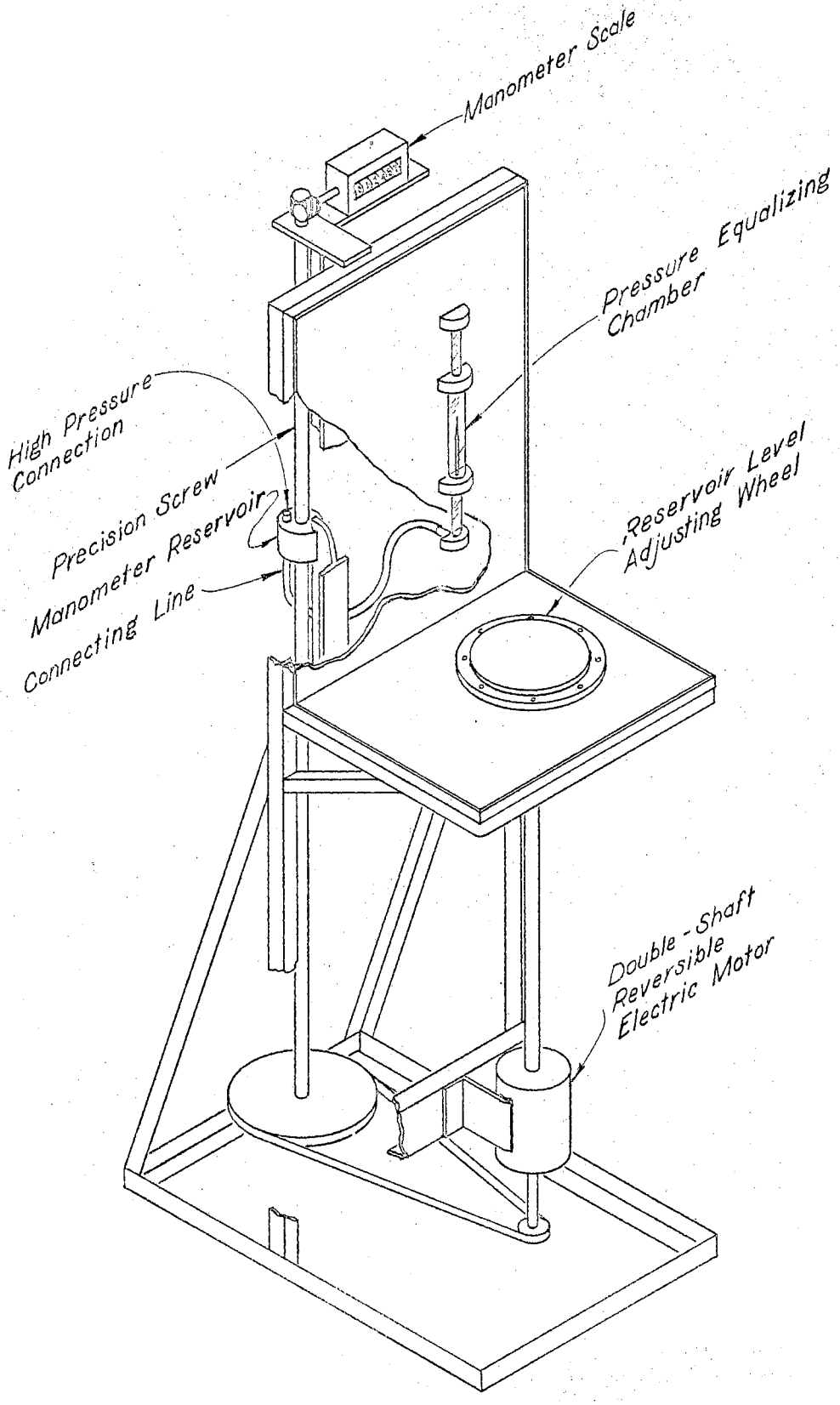

Figure 8. Oklahoma State University Micromanometer

manometer scale since one inch of travel of the reservoir is indicated by 100 counts on the counter.

The shaft is lowered until the meniscus of the water is again touching the reference needle. The manometer scale then is indicating the unknown pressure to the nearest hundredth of an inch.

To permit a more accurate adjustment, a double shaft motor was selected so that changes in the reservoir level could be made without operating the motor. An extension was placed on this extra shaft and attached to a wheel on the manometer stand. By turning this wheel, the screw may be turned in either direction to raise or lower the reservoir level.

The only inaccuracy in the system, other than the experience of the operator, is in the threaded shaft upon which the accuracy of the measurements depend. For future models a precision ball-screw will be used which has a maximum error of one-thousandth of an inch in ten feet of travel. In this manner the hysteresis effects and manufacturing inaccuracies will be reduced to a minimum.

APPENDIX B

PREPARATION OF DATA USING THE DIGITAL COMPUTER

The determination of the filter capacity constant, C_f, from equation (4-7), required several lengthy calculations. For this reason the decision was made to make use of the I.B.M., 650, digital computer. Also, through using the computer, an unbiased and accurate analysis of the pressure drop versus flow rate data could be obtained.

The first function of the computer program was to calculate the weight rate of flow at each test point from equation (5-1). This in itself was not difficult except for the selection of an appropriate value for the coefficient of discharge for the flow nozzle. This coefficient is a function of the differential pressure across the flow nozzle and the temperature of the flowing air. It is expressed in the form of a graph in an A.S.M.E. Power Test Code (12). Since the temperature of the air varied only slightly during the series of tests, it was assumed to be a constant in order to simplify the determination of a nozzle coefficient equation. Having done this, it was possible to define the coefficient by the following equation:

$$C_n = \frac{\text{Ln}P_w * 144.20837}{151.2924} \quad . \qquad \text{(B-1)}$$

After solving for the respective flow rates, the second func-

tion required of the program was to use some averaging method to construct the best straight line through the group of data points. The least-squares fitting method, as outlined in Amyx, et al. (13), was chosen to accomplish this. Using this method, the parameters associated with the "optimum" straight line could be obtained using the following equations:

$$m = -\frac{\sum_{i=1}^{n} LnW_i \sum_{i=1}^{n} LnP_{fi} - n \sum_{i=1}^{n} (LnW_i)(LnP_{fi})}{n \sum_{i=1}^{n} (LnW_i)^2 - \left\{\sum_{i=1}^{n} LnW_i\right\}^2}, \quad \text{(B-2)}$$

$$b = \frac{\sum_{i=1}^{n} LnP_{fi} \sum_{i=1}^{n} (LnW_i)^2 - \sum_{i=1}^{n} (LnW_i)(LnP_{fi}) \sum_{i=1}^{n} (LnW_i)}{n \sum_{i=1}^{n} (LnW_i)^2 - \left\{\sum_{i=1}^{n} LnW_i\right\}^2}, \quad \text{(B-3)}$$

and

$$s = \left\{\frac{1}{n} \sum_{i=1}^{n} (LnP_{fi} - LnP_{ci})^2\right\}^{1/2}. \quad \text{(B-4)}$$

The completed program (Table III) was written so that up to seven flow rate and pressure drop data points could be used in the calculation of slope and intercept data for a given filter. To permit this, it was necessary that the data enter the computer on three separate data cards for a single test. The first of these cards contained the flow rates for the individual test, and the second card contained the respective pressure drop readings.

TABLE III

FORTRAN PROGRAM FOR THE I.B.M., 650, DIGITAL COMPUTER

Step No.	Operation

```
001000DIMENSIONFLOWP(7),FILTP(7),C(7
001001),W(7),ALOGW(7),FPLOG(7),CURVP
001002(7),DELTA(7)
000010READ,FLOWP
000020READ,FILTP
000030READ,IDEN,BUBP,D,PB,TA,N,BLPNT
001010SUMFP=0.0
001020SUMW=0.0
001030SUMWF=0.0
001040SUMW2=0.0
001050SUMDL=0.0
000040DO12I=1,N
000050C(I)=(LOGEF(FLOWP(I))+144.208
0000517)/151.2924
000060W(I)=6.87*C(I)*D*D*((PB*FLOWP
0000611)/TA)**0.5)
000070ALOGW(I)=LOGEF(W(I))
000080FPLOG(I)=LOGEF(FILTP(I))
000090SUMFP=SUMFP+FPLOG(I)
000100SUMW=SUMW+ALOGW(I)
000110SUMW2=SUMW2+(ALOGW(I))**2.0
000120SUMWF=SUMWF+ALOGW(I)*FPLOG(I)
001060NA=N
000130AN=N
000140SLOPE=(SUMW*SUMFP-AN*SUMWF)/(A
000141N*SUMW2-SUMW*SUMW)*(-1.0)
000150ENDPT=(SUMFP*SUMW2-SUMWF*SUMW
000151/(AN*SUMW2-SUMW*SUMW)
000160DO19J=1,NA
000170CURVP(J)=ENDPT+SLOPE*ALOGW(J)
000180DELTA(J)=(FPLOG(J)-CURVP(J))*
0001812.0
000190SUMDL=SUMDL+DELTA(J)
000200SDEV=(SUMDL/AN)**0.5
000210PUNCH,IDEN,BUBP,SLOPE,ENDPT,S
000211EV,BLPNT
000220GOTO1
000230END
```

The third data card contained the additional information necessary to calculate the rates of flow, namely, the absolute temperature of the flowing air, the barometric pressure at the time of the test, and the diameter of the nozzle being used. In addition to this data, the data on the third card included an identification number, a statement of the number of points to be averaged, and also two test readings indicating the sizes of the pores in the element. These additional readings were the "bubble point" and the "boiling point" for the given filter. These two test readings were also included on the answer card along with the filter identification number and the characteristics of the straight line curve as determined from the least squares method.

APPENDIX C

CONTAMINANT CAPACITY TEST PROCEDURES

The most reliable method of determining the contamination level of a filter element is to submit the element to a contamination or "dirt" capacity test. The purpose of this test is to discover the weight of a standard contaminant which a filter will "hold" before the pressure differential across the element reaches a given value. In this manner it is possible to gain an insight into the relative contamination levels of a group of filter elements. Because this type of test is widely used, it was selected as the means for correlating the Air Permeameter test results.

The contamination capacity tests were conducted on the filter evaluation test stand. (14). This stand (Figure 9) is equipped to conduct, not only these tests, but also hydraulic pressure drop versus flow rate tests. As may be noted on the circuit schematic (Figure 10), the test stand is equipped with several methods by which the contamination concentration of the test fluid may be maintained. Such control is mandatory in this type of experiment in order to insure that the only particles being trapped by the test filter are those which are added artificially.

The control methods included the use of an auxilliary test stand equipped with a hydroclone, a nonbarrier filtration device. During testing, the fluid was continuously circulated through this

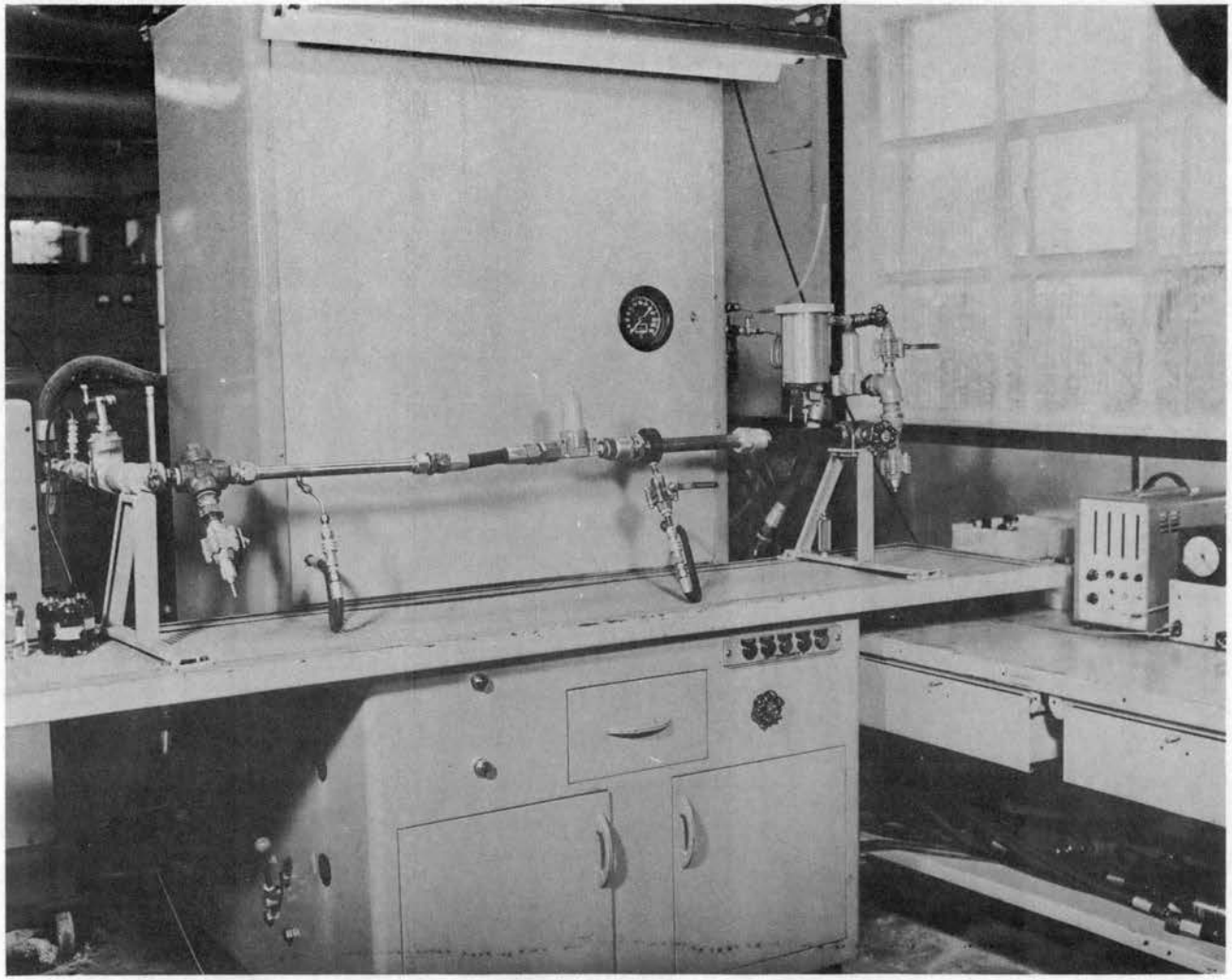

Figure 9. Filter Evaluation Test Stand.

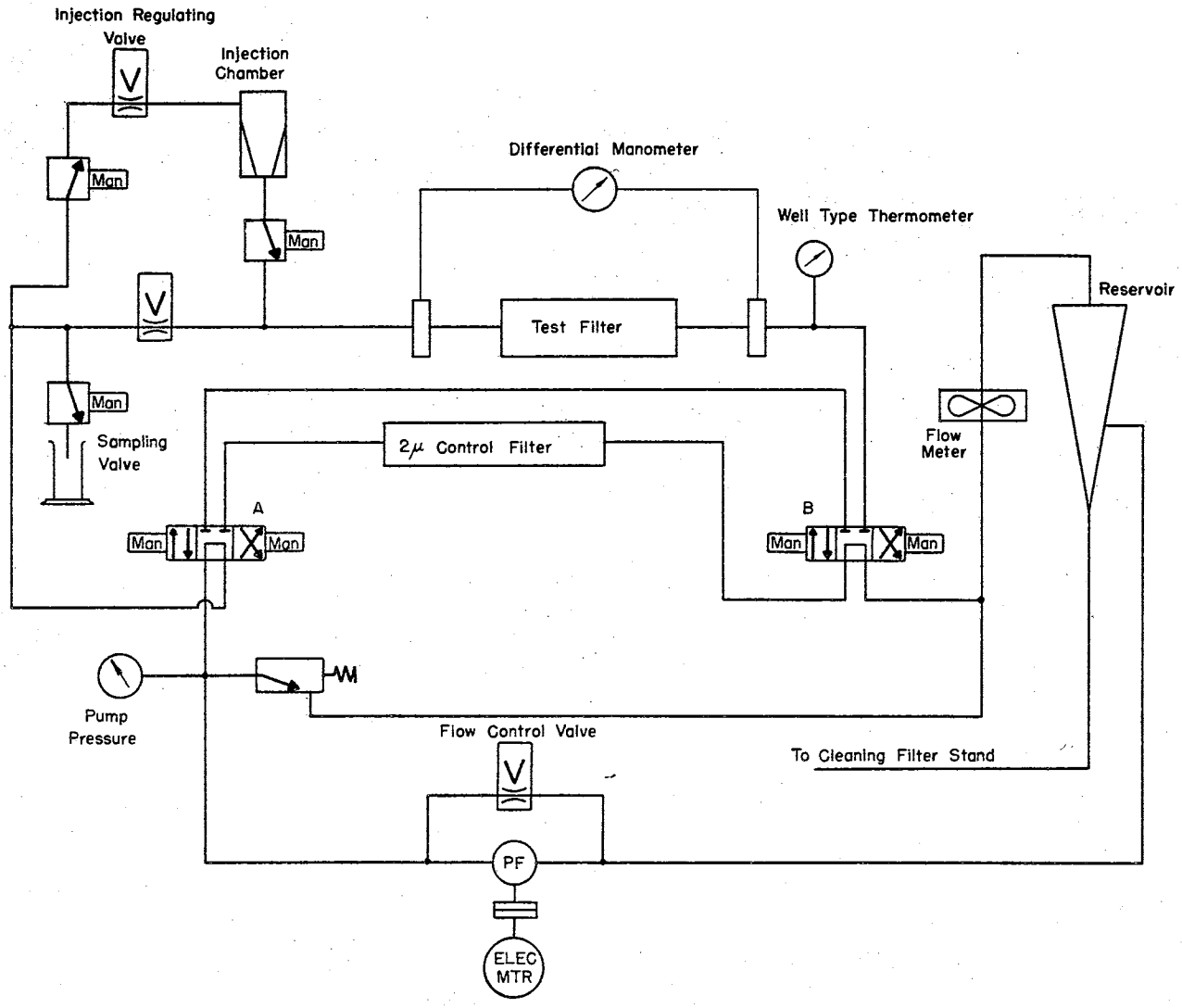

Figure 10. Schematic Diagram of Filter Evaluation Stand

system to help maintain the contamination of the reservoir fluid at a low level. A one-half micron nominal, 2-micron absolute control filter was installed preceeding the test section to further improve the quality of the fluid. Another important phase of the control techniques in this area was the use of a specially designed conical reservoir. The purpose of the reservoir was to eliminate the possibility of reservoir "dead zones", or regions in the reservoir where particles might collect. By placing the suction line to the auxilliary filtration stand in the apex of the cone, particles in the hydraulic oil were kept in suspension and subject to removal by one of the two filtering media.

In performing the contaminant capacity tests, samples of a standardized fine, air cleaner test dust (Figure 11) were weighed on an analytical balance in .3gm, .2 gm, and .1 gm sizes. The weighed samples were then placed in 100 milliliter sample bottles which had been cleaned of foreign contamination. The bottles were then filled with hydraulic fluid and, prior to each test, were shaken in the bath of an ultrasonic cleaner to disperse the particles. This was done to provide a uniformly contaminated sample.

For a test the element was placed in its housing and a measurement taken of the differential pressure across this assembly at the rated flow of the filter. A contaminated sample was then poured into the injection chamber and the chamber resealed. The opening of two ball valves caused a portion of the fluid upstream from the test element to be diverted into the top of the conical-shaped injection chamber and out through the apex of the cone.

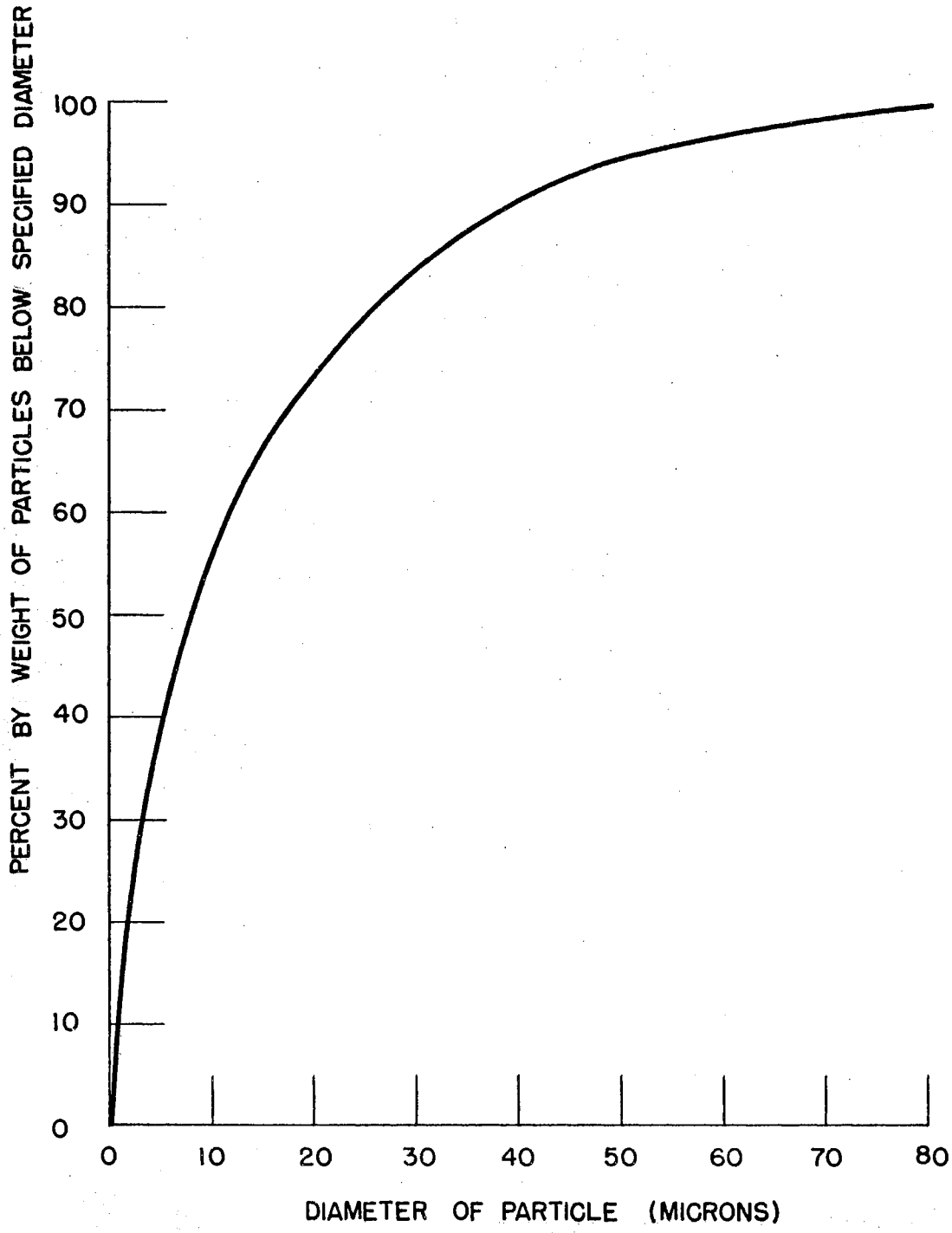

Figure 11. Particle Size Distribution Curve for AC Fine Test Dust

The shape of this chamber was chosen to be conical so that all of the injected sample might reach the test element. Upon leaving the chamber the fluid passed through a ball valve into a one-quarter inch diameter stainless steel tube. The tube, in turn, extended into the center of the principle flow line preceeding the test filter.

After circulating through the injection system for a period of one and one-half minutes, flow was again shut off to this system and another injection was prepared. One minute after the closure of the injection circuit the differential pressure across the element and housing was measured. This time interval was necessary to allow for the response of the sensitive manometer being used to record the pressure drop.

After recording the pressure drop after the first injection, the second injection was begun. The procedure was then repeated until the differential pressure across the test assembly reached a predetermined value. For the 12 gpm elements this reference pressure was 58.5 psi or 40 psi higher than the pressure drop across the test run and the empty housing. For the 8 gpm elements the chosen differential was also 58.5 psi or 50 psi higher than the housing pressure drop.

The contaminant capacity (Figure 12) for these tests was then defined as the weight of test dust which was required to cause the differential pressure across the element to reach the reference value. It should be noted that while the contaminant capacity is based on the total weight of test dust added to the fluid upstream from the filter, a considerable portion of the

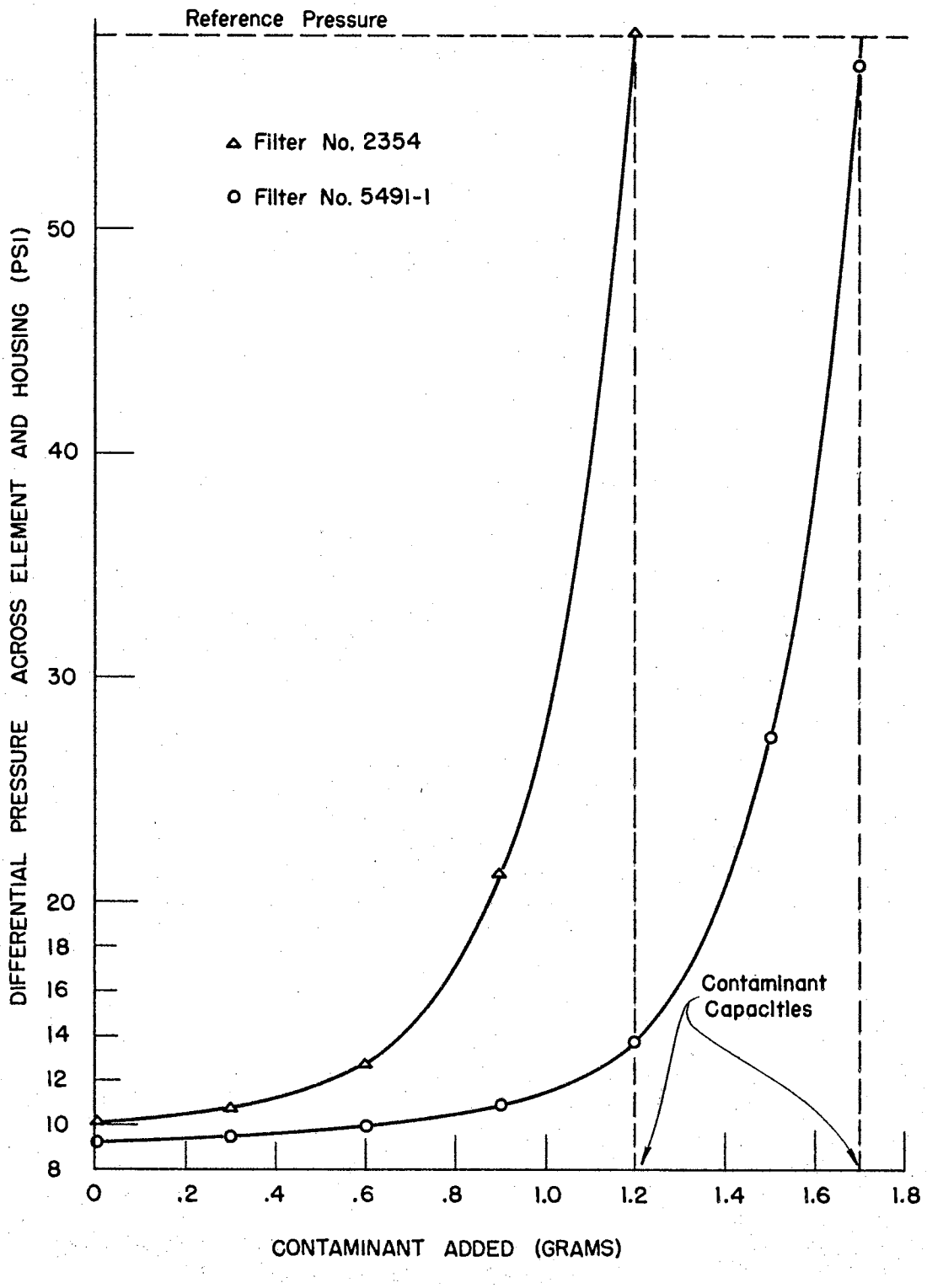

Figure 12. Contaminant Capacity Curves

contaminant passes through the element because it is smaller than the pores in the wire cloth.

APPENDIX D

LIST OF SYMBOLS AND ABBREVIATIONS

a	Empirical constant in Rainard's constant, C_1, (2-6), dimensionless.
A	Total area of filter, $cm.^2$
A_p	Area of individual pore, $cm.^2$
b	Value of $Ln(P_f)$ at $Q_f = 0$.
C	Constant in equation (2-11), gpm per lb.
C_f	Filter capacity constant.
C_n	Flow nozzle coefficient, dimensionless.
C_1	Initial coefficient in Rainard's equation, (2-5), gm. $sec.^2$ per $cm.^8$.
C_2	Viscous coefficient in Rainard's equation, (2-5), gm. sec. per $cm.^5$.
D_m	Diameter of largest pore in filter medium, microns.
D_n	Diameter of A.S.M.E. flow nozzle, in.
$D(R)$	Frequency-distribution function of pore size in equation (2-3), $cm.^3$ pore volume per $cm.^3$ solid per micron size interval.
$\frac{dp}{dl}$	Pressure gradient in Darcy's equation, (2-4), atmospheres per cm.
g_c	Conversion factor in Newton's Law of Motion, 980 gm. cm. per gm. force per $sec.^2$.

k	Exponent in equation (2-11), dimensionless.
K	Permeability in equation (2-4), darcys.
K_1	Flow constant in equation (2-9), cm.
K_2	Constant in equation (4-1), characteristic of units employed.
L	Effective pore length, cm.
m	Slope of $Ln(P_f)$ versus $Ln(Q_f)$ curve.
n	Number of pores in filter medium.
n	Number of data points in equations (B-2), (B-3), and (B-4).
N	Number of pores per unit area.
$\bar{P}$	Absolute pressure at filter medium, psi.
P_a	Atmospheric pressure, in. of Hg.
P_b	Pressure drop across unused medium when first bubble of gas is passed, in. of water.
P_c	Pressure calculated using curve obtained by least square's method, in. of water.
P_f	Differential pressure across filter element.
P_w	Differential pressure across A.S.M.E. flow nozzle, in. of water.
$\triangle P$	Differential pressure across filter medium, psi.
Q	Rate of flow through porous medium, $cm.^3$ per sec.
Q_f	Rate of flow through filter element.
R	Pore radius, microns.
s	Exponent in equations (4-1), (4-2), and (4-3), dimensionless.

S	Average deviation of data points from calculated curve, in. of water.
T_a	Absolute temperature of flowing air, degrees Rankine.
V	Fluid velocity in porous medium, cm. per sec.
V_o	Volume of fiber solids in test specimen, $cm.^3$.
$d(\triangle V)$	Slope of pressurizing curve at pressure $\overline{P}$ in equation (2-3), $cm.^3$ pore volume per $cm.^3$ fiber per psi.
W	Weight rate of air flow, lb. per min.
θ	Theta, advancing contact angle of liquid with surface in equation (2-1), degrees.
μ	Mu, viscosity of fluid, centipoise.
ρ	Rho, density of liquid absorbate in equation (2-6), gm. per $cm.^3$.
σ	Sigma, surface tension of bubble test liquid in equation (2-1), dynes per cm.

ABBREVIATIONS

cm.	Centimeter, centimeters
gm.	Gram, grams
gpm	Gallons per minute
in.	Inch, inches
lb.	Pound, pounds
min.	Minute, minutes
psi	Pounds per square inch
sec.	Second, seconds

APPENDIX E

APPARATUS AND EQUIPMENT

1. Air Permeameter: Model 1 designed and built by the School of Mechanical Engineering, Oklahoma State University.

2. Digital Computer: Manufacturer, International Business Machines Corporation; Model 650.

3. Filter Evaluation Test Stand: Designed and built by the School of Mechanical Engineering, Oklahoma State University.

VITA

Roger Harrell Tucker

Candidate for the Degree of

Master of Science

THESIS: THE DEVELOPMENT OF A METHOD TO PREDICT THE CONTAMINANT CAPACITIES OF LOW MICRON, WOVEN STAINLESS STEEL FILTER ELEMENTS

MAJOR FIELD: Mechanical Engineering

BIOGRAPHICAL:

Personal Data: Born July 30, 1939, in Wichita, Kansas, the son of Clyde and Winston Tucker.

Education: Graduated from Putnam City High School, Oklahoma City, Oklahoma in 1957; received the Bachelor of Science degree from Oklahoma State University, with a major in Mechanical Engineering, in May, 1961; completed the requirements for the Master of Science degree in May, 1963.

Experience: Employed as a Research Assistant in the School of Mechanical Engineering, Oklahoma State University, from February, 1961 to September, 1962.

Honorary Organizations: Pi Tau Sigma, Omicron Delta Kappa.

Honors and Awards: Who's Who Among Students in American Universities and Colleges, 1960-1961.